# Atomic disorder and phase transformation in intermetallic compounds of the type $T_3X_2$ ($T$=Ni,Fe,Mn; $X$=Sn,Ge) by mechanical milling

G. F. Zhou and H. Bakker
*Van der Waals-Zeeman Laboratorium, Universiteit van Amsterdam, Valckenierstraat 65, 1018 XE Amsterdam, The Netherlands*
(Received 9 July 1993; revised manuscript received 11 November 1993)

The structural development of the ordered intermetallic compounds $T_3X_2$ ($T$=Ni,Fe,Mn; $X$=Sn,Ge) upon mechanical milling was investigated by x-ray diffraction, magnetic measurements, and subsequently by differential scanning calorimetry (DSC). It is found that the magnetization at 4.2 K increases continuously with increasing milling time in ferromagnetic $Ni_3Sn_2$ and $Fe_3Ge_2$. In contrast, in ferrimagnetic $Mn_3Sn_2$ it decreases. The unit-cell volume of both $Mn_3Sn_2$ and $Fe_3Ge_2$ continuously increases. These results are explained well in terms of a special type of atomic disorder: redistribution of transition-metal atoms over two different types of transition-metal sites, induced by ball milling. Exothermic heat effects corresponding to atomic reordering are observed in the DSC scans of $Mn_3Sn_2$ and $Fe_3Ge_2$ as well as $Ni_3Sn_2$ after various periods of milling. The heat evolved in the atomic reordering process increases gradually with milling time. After long-time milling all physical parameters tend to become constant. After prolonged periods of milling, a phase transformation in $Ni_3Sn_2$ from the orthorhombic-structure low-temperature phase (LTP) to the hexagonal-structure high-temperature phase (HTP) is observed accompanied by a sharp increase in magnetization. $Mn_3Sn_2$ and $Fe_3Ge_2$ remain in the hexagonal structure. The exothermic heat effect corresponding to the phase restoration of the ball-milled metastable HTP to the original equilibrium LTP is evident from DSC scans of $Ni_3Sn_2$ after long milling periods. The occurrence of the ball-milling-induced phase transformation in $Ni_3Sn_2$ is also confirmed by a comparison of the ball-milled phase to the high-temperature phase obtained by rapid quenching. The excellent agreement of all experimental results obtained by different techniques proves that by mechanical milling well-defined metastable states are generated in these $B8$-like compounds and that atomic disorder is the main source of energy storage during ball milling of intermetallic compounds. The particular type of atomic disorder in these $B8$-like compounds cannot be obtained by rapid quenching from high temperatures.

## I. INTRODUCTION

Mechanical milling of initially ordered intermetallic compounds may transform the compound to amorphous[1–4] or to a solid solution.[5] Since those states have a higher free energy than the starting material, defects introduced during milling must be responsible for raising the free energy. What type of defects can provide the required increase in free energy is still a subject of debate and investigation. In most theoretical work it is stated that atomic (chemical) disorder is the main source of energy storage.[6–8] Atomic disorder during the early stage of ball milling was really detected in $NiTi_2$ by differential scanning calorimetry,[9] in $Ni_3Al$ by x-ray diffraction,[10] in $A15$ compounds by following the degradation of the superconducting transition temperature,[11,12] and in $B2$ CoGa and CoAl by an increase of the magnetization and a decrease of the lattice parameter.[13,14] The type of atomic disorder turned out to be characteristic of the specific compound. Antisite disorder was found in the $A15$ compounds and triple-defect disorder in CoGa and CoAl. It was assessed that in these compounds the effect of ball milling is similar to that of irradiation or of high temperature.

In the present paper, we report a systematic study of the behavior of the intermetallic compounds $Ni_3Sn_2$, $Fe_3Ge_2$, and $Mn_3Sn_2$ with a $B8$-like structure. The compounds $Fe_3Ge_2$ and $Mn_3Sn_2$ and the high-temperature phase (HTP) of $Ni_3Sn_2$ are $B8_2$ type. This structure is hexagonal and is shown in Fig. 1. The large filled circles represent the atoms of the nontransition element, whereas the small open and filled circles represent two different types of interstitial positions that can be occupied by transition-metal atoms: octahedral (I) and tetrahedral (II) interstices. The octahedral sites are fully occupied, whereas the tetrahedral sites are only half occupied. The as-prepared $Ni_3Sn_2$ [low-temperature phase (LTP)] crystallizes in an orthorhombic structure, which exists from room temperature up to 873 K. At this temperature the orthorhombic LTP transforms to the hexagonal HTP by a slight shift in the positions of atoms. In

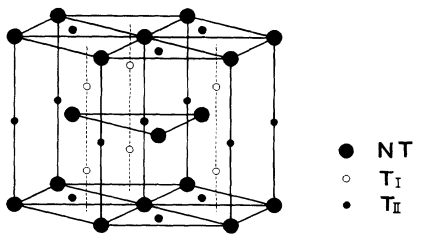


FIG. 1. Hexagonal $B8_2$ structure: large filled circles are the non-transition-metal atoms (NT); small open circles are type-I sites; and small filled circles are type-II sites.

 

our previous investigations,[15,16] it was found by x-ray diffraction and magnetic measurements that in all compounds mechanical milling redistributes the transition-metal atoms over I and II sites. This means a so far unknown type of atomic disorder. Moreover, it turned out that after prolonged milling of $Ni_3Sn_2$ a phase transformation from the orthorhombic structure to the $B8_2$-type hexagonal structure occurs. We now present results mainly obtained by differential scanning calorimetry (DSC). These results provide further evidence for the atomic disorder and phase transformations. Moreover, an explanation of the variation of Curie temperature during ball milling is given. A comparison is made with previous results.

## II. EXPERIMENTAL PROCEDURE

The starting compounds $T_3X_2$ were prepared by arc melting of weighted amounts of pure transition metal ($T$) and nontransition metal ($X$) in a purified argon atmosphere. In order to obtain a homogeneous single-phase sample, the arc-melted button was wrapped in tantalum foil, then sealed in a quartz tube under argon atmosphere, and annealed at 600°C for 10 days in the case of $Mn_3Sn_2$, at 800°C for 5 days in the case of $Fe_3Ge_2$, and at 500°C for 4 days in the case of $Ni_3Sn_2$. The x-ray-diffraction patterns of the annealed samples show single phases. The compound $Ni_3Sn_2$ for the quenching experiment was obtained in the same way as described above. Rapid quenching of the $Ni_3Sn_2$ from various temperatures ranging from 700 to 900°C was performed in a self-designed low-temperature powder-quenching device[17] to obtain the high-temperature phase of $Ni_3Sn_2$. The cooling rate is about $10^4$ K/s. The ball milling was carried out in a hardened steel vial and, in order to prevent reactions with oxygen or nitrogen, in a vacuum of about $10^{-6}$ Torr.[15] The starting amount of material was a few grams. Powders for x-ray diffraction and magnetic measurements were taken from the samples milled for different periods under argon atmosphere in a glovebox and after that the powder was used for DSC measurement. X-ray-diffraction patterns were taken at room temperature by means of a Philips diffractometer with vertical goniometer using Cu $K\alpha$ radiation. For an accurate measurement of the lattice parameters the powder sample was mounted on the sample holder with silicon as a standard. The temperature dependence of the magnetization was measured from room temperature to liquid-helium temperature in a self-constructed magnetometer. The sensitivity of this magnetometer is better than $10^{-5}$ A m$^2$. The high-field magnetization measurements at 4.2 K were performed in the Amsterdam High Field Installation[18] in which magnetic fields up to 40 T can be generated in a semicontinuous way. A stepwise field profile up to 21 T (one up to 35 T) was used. The sensitivity of this installation is about $10^{-5}$ A m$^2$. Differential scanning calorimetry measurements were carried out in a Perkin-Elmer DSC-7 in argon gas flux at a speed of 30 cm$^3$/min to protect the sample against oxidation. A heating rate of 10 K/min was used in the DSC scan. The scan was repeated twice for each sample. The temperature and the reaction heat were calibrated by pure indium and zinc standards.

## III. EXPERIMENTAL RESULTS

### A. Milling of hexagonal $Mn_3Sn_2$

It was derived from the x-ray-diffraction pattern that the as-prepared $Mn_3Sn_2$ belongs to the $B8_2$-type hexagonal structure having the space group $P6_3/mmc$ with some superlattice reflections. The superlattice reflections are attributed to the long-range-ordered arrangement of the holes and Mn atoms on the II sites of the $B8_2$ structure. During ball milling, the intensity of all superlattice reflections decreases and these reflections as well as two "fundamental" peaks eventually disappear. Details of the change of the x-ray-diffraction patterns during ball milling have been reported in Ref. 16. The lattice parameters were derived from the x-ray-diffraction patterns of $Mn_3Sn_2$ after various periods of milling. Figure 2 gives the unit-cell volume of $Mn_3Sn_2$ as a function of milling time. It is clear that the unit-cell volume of $Mn_3Sn_2$ increases continuously with increasing milling time and becomes nearly constant after 60 h of milling. The relative increase is about 1.3%. Due to the refinement of crystallite size and the development of stresses, the Bragg peaks become broader upon milling. Based on the width of the Bragg peaks, the crystallite size is estimated after correction for internal-strain broadening (using Langford's Voigt-deconvolution method) and is plotted in Fig. 3 as a function of milling time. The crystallite size of $Mn_3Sn_2$ decreases with increasing milling time. The final value of the average crystallite size is about 5–6 nm. This means that a nanocrystalline structure is also formed during the late stage of milling.

The field dependence (up to 21 T) of the magnetization at 4.2 K of $Mn_3Sn_2$ after various periods of milling is shown in Fig. 4. For a sample milled for 80 h an external magnetic field up to 35 T was applied. The magnetization at 21 T taken from the various magnetization curves is plotted in Fig. 5 as a function of milling time. The

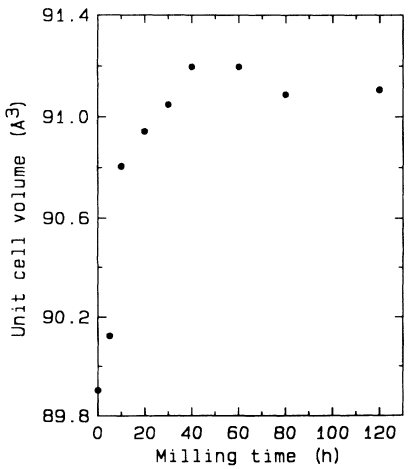


FIG. 2. Unit-cell volume of $Mn_3Sn_2$ as a function of milling time.

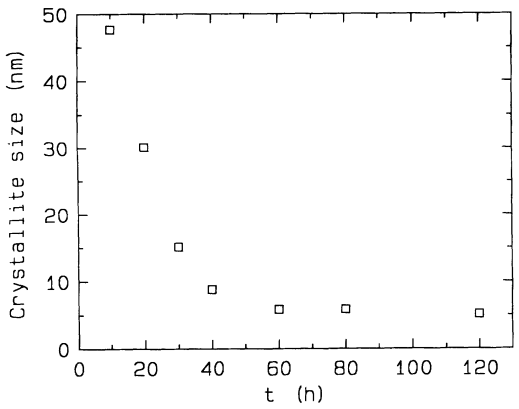


FIG. 3. Average crystallite size of $Mn_3Sn_2$ as a function of milling time.

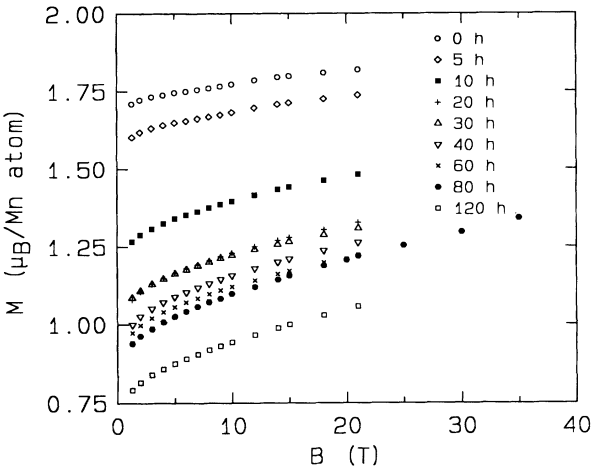


FIG. 4. High-field magnetization curves at 4.2 K of $Mn_3Sn_2$ after various periods of milling.

magnetization decreases continuously with increasing milling time for milling periods shorter than 60 h. Upon further milling the magnetization decreases gradually and tends to become constant. After 120 h of milling, the magnetization drops again. The temperature dependence of the $Mn_3Sn_2$ after various periods of milling was measured in an external field of 0.5 T. The Curie temperature $T_C$ derived from the corresponding $M^2$-$T$ curves is plotted in Fig. 6 as a function of milling time. Arrot pots were used to confirm the transition temperature. It is clearly seen that in the early stage of milling the $T_C$ value decreases gradually with increasing time. After 60 h of milling, the $T_C$ value tends to become constant.

The DSC scans of all ball-milled $Mn_3Sn_2$ samples show at least two pronounced exothermic transitions. In most samples even three exothermic heat effects are observed. Figure 7 shows three typical DSC scans of $Mn_3Sn_2$ at a heating rate of 10 K/min after 10, 30, and 40 h of milling. These exothermic transitions are irreversible, which means that after heating to high temperature the exothermic peaks do not appear upon reheating. The total heat evolved in these transitions is plotted in Fig. 8 as a function of milling time. It is clear that the transition heat increases gradually with increasing milling time. After 60 h of milling it tends to become constant at a value of about 4 kJ/mol.

For a better understanding of these exothermic transitions $Mn_3Sn_2$ milled for 30 h was heated in the DSC at a heating rate of 10 K/min to different temperatures and subsequently cooled down to room temperature at a speed of 200 K/min. The corresponding x-ray-diffraction patterns are given in Fig. 9. The pattern labeled 433 K, the peak temperature of the first exothermic transition, shows a few extra diffraction peaks and sharper peaks in comparison to the pattern of the ball-milled $Mn_3Sn_2$. For the sample heated to 553 K, the end of the second transition peak, an increase of the intensity of the x-ray-diffraction patterns of the long-range-ordered $Mn_3Sn_2$ (as prepared) is observed. Upon further heating to 603 K, the end of the third transition peak, all the peaks in x-ray-diffraction pattern become somewhat sharper than those in the sample heated up to 553 K. A number of heating rates, 5, 10, and 20 K/min, were applied to mea-

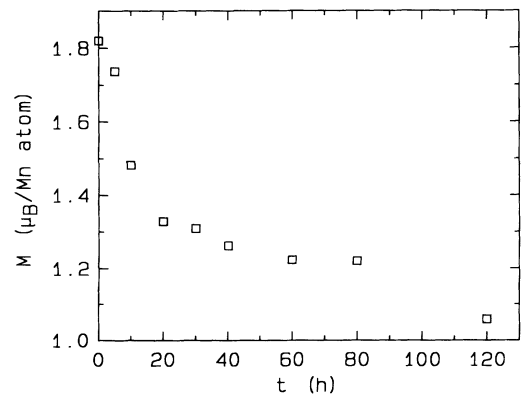


FIG. 5. Magnetization at 4.2 K of $Mn_3Sn_2$ at 21 T as a function of milling time.

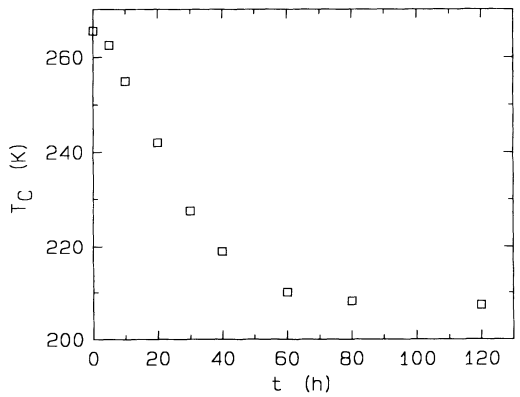


FIG. 6. Curie temperature of $Mn_3Sn_2$ as a function of milling time.

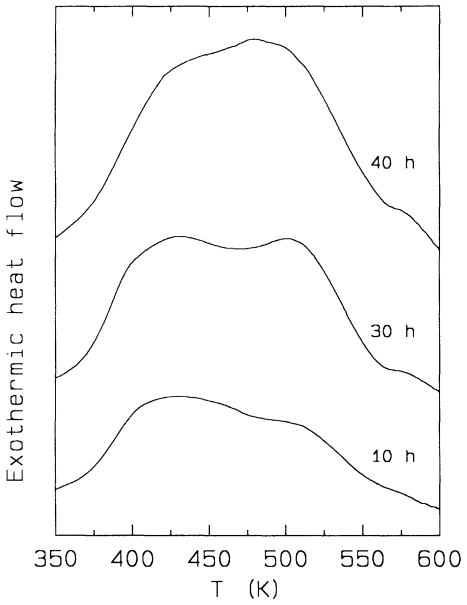


FIG. 7. Typical DSC scans of $Mn_3Sn_2$ after 10, 30, and 40 h of milling.

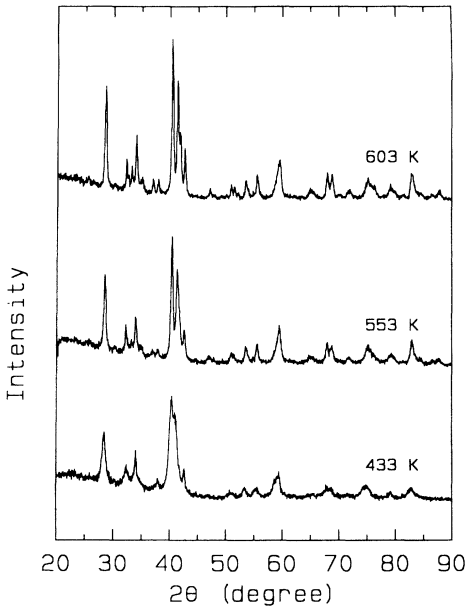


FIG. 9. X-ray-diffraction patterns of $Mn_3Sn_2$ milled for 30 h after heating in the DSC to 433, 553, and 603 K and subsequently cooling to room temperature with a cooling rate of 200 K/min.

sure the dependence of the peak temperatures on heating rate. The Kissinger[19] plots are displayed in Fig. 10. The activation energies for the first and second peaks are 174 and 102 kJ/mol, respectively.

### B. Milling of hexagonal $Fe_3Ge_2$

The x-ray-diffraction pattern of the as-prepared $Fe_3Ge_2$ is also characteristic of the $B8_2$-type hexagonal structure. During milling the intensity of all the Bragg peaks decreases and some peaks eventually disappear. Values of the lattice parameters were derived from the x-ray-diffraction patterns. Figure 11 displays the unit-cell volume of $Fe_3Ge_2$ as a function of milling time. It is clear that the unit-cell volume of $Fe_3Ge_2$ increases gradually and becomes constant after 140 h. The relative increase is about 1.2%, the same magnitude as in $Mn_3Sn_2$. The crystallite size of $Fe_3Ge_2$ decreases with milling time in the early stage and reaches a constant value of approximately 14 nm after milling longer than 140 h.

The magnetization at 21 T as a function of milling time is shown in Fig. 12. The values of the magnetization were taken from the various high-field magnetization curves at 4.2 K as in $Mn_3Sn_2$. It is clear that the magnetization of $Fe_3Ge_2$ increases continuously with milling time up to 140 h. Upon further milling the magnetization tends to become constant.

As for $Mn_3Sn_2$, three exothermic heat effects are observed in the DSC scans after various periods of milling. The total heat evolved in the exothermic transitions is

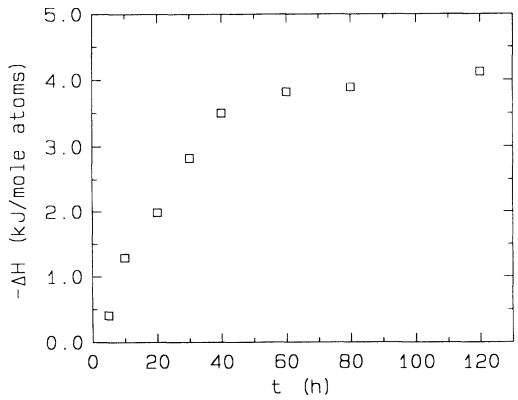


FIG. 8. Total heat evolved in the exothermic reaction (the sum of the three exothermic peaks) in $Mn_3Sn_2$ as a function of milling time.

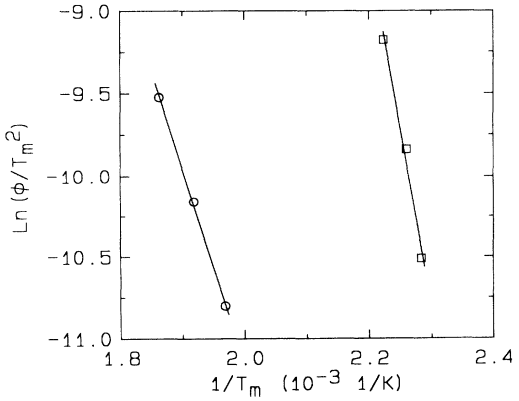


FIG. 10. Kissinger plots of the first (squares) and second (circles) exothermic peaks in $Mn_3Sn_2$ milled for 30 h in DSC. $\phi$ is the heating rate and $T_m$ the peak temperature.

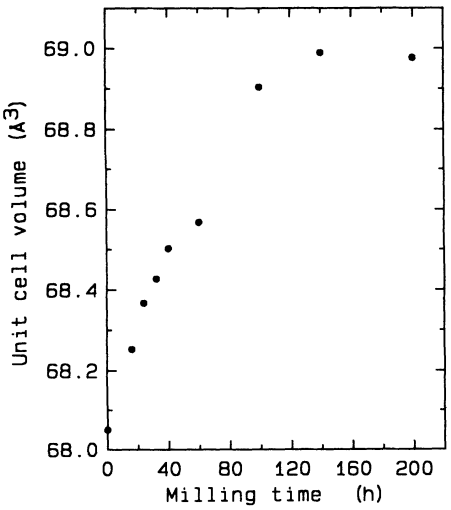


FIG. 11. Unit-cell volume of $Fe_3Ge_2$ as a function of milling time.

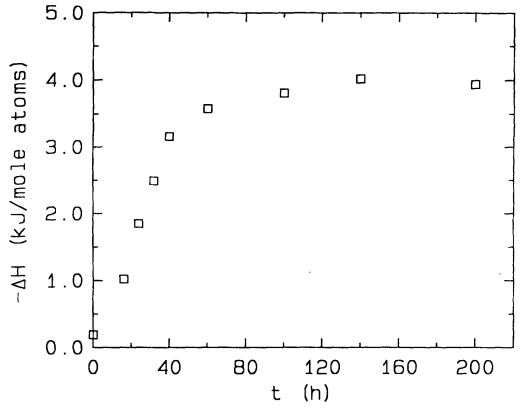


FIG. 13. Total heat evolved in the exhermic reactions (the sum of the three exothermic peaks) in $Fe_3Ge_2$ as a function of milling time.

given in Fig. 13 as a function of milling time. It is seen that the heat released in the exothermic transitions increases with milling time. After 140 h of milling, it tends to become constant with a value of about 4 kJ/mol. The Curie temperature of the starting material was obtained from DSC. It is about 430 K. This is in good agreement with the value reported in the literature.[20] The fact that the ferromagnetic-paramagnetic transition overlaps with the atomic reordering peak makes an accurate determination of the Curie temperature difficult. Therefore, high-temperature dc magnetic-susceptibility measurements in a Faraday balance are currently being undertaken.

### C. Milling of orthorhombic $Ni_3Sn_2$

Figure 14 shows the x-ray-diffraction patterns of $Ni_3Sn_2$ after 0 and 100 h of milling as well as of $Ni_3Sn_2$ quenched from 1073 K (HTP). In agreement with Ref. 21, all peaks in the x-ray-diffraction pattern of as-prepared $Ni_3Sn_2$ (0 h) can be identified as belonging to the low-temperature phase (LTP) with the $Ni_3Sn_2$-type orthorhombic structure (space group *Pnma* ). The x-ray pattern of $Ni_3Sn_2$ quenched from 1073 K is characteristic of the high-temperature phase with $B8_2$-type hexagonal structure, which exists in the phase diagram above 873 K.[22] This structure is the same as that of $Mn_3Sn_2$ and $Fe_3Ge_2$. For milling periods up to 32 h, the material remains in the orthorhombic structure of the LTP. However, the x-ray-diffraction patterns of $Ni_3Sn_2$ milled for periods from 40 to 100 h show the characteristics of the $B8_2$-type hexagonal structure of the HTP. Details of the change of the x-ray-diffraction pattern of $Ni_3Sn_2$ during ball milling have been reported in Ref. 15. It is clear from Fig. 14 that $Ni_3Sn_2$ after 100 h of milling has the same structure as quenched $Ni_3Sn_2$. This means that ball milling induces a phase transformation from the orthorhombic structure to the hexagonal structure as expected from the phase diagram. The absence of (100) and (203)

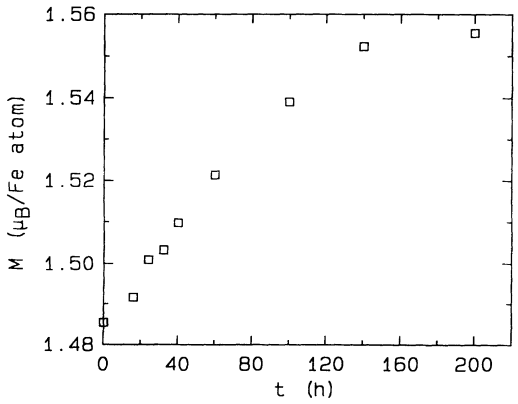


FIG. 12. Magnetization at 4.2 K of $Fe_3Ge_2$ at 21 T as a function of milling time.

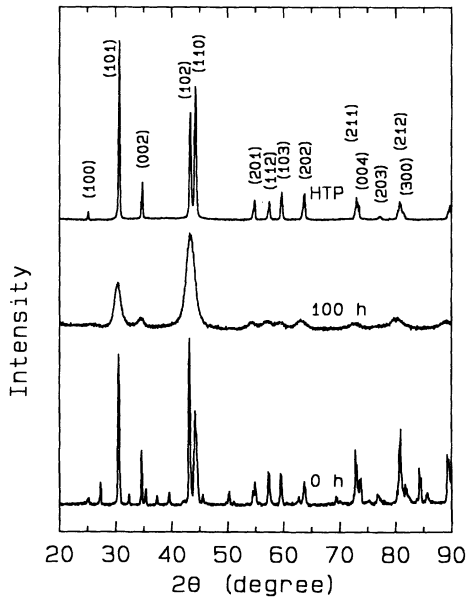


FIG. 14. X-ray-diffraction patterns of $Ni_3Sn_2$ after 0 and 100 h of milling as well as of $Ni_3Sn_2$ quenched from 1073 K (HTP).

reflections in the ball-milled HTP indicates that the HTP obtained by ball milling is atomically disordered. The broad character of the diffraction peaks in the ball-milled HTP is attributed to the refinement of crystallite size and the development of strains during ball milling.

The magnetization at 21 T as a function of milling time is shown in Fig. 15. The filled circle at zero hour of milling is for $Ni_3Sn_2$ quenched from 1073 K. The magnetization of the HTP is larger than that of the as-prepared LTP and the magnetization of the LTP increases continuously with milling time up to 32 h. A drastic increase in magnetization is observed after 40 h of milling. Upon further milling the magnetization tends to become constant. The magnetization of the ball-milled HTP is much larger than that of the HTP obtained by quenching. The Curie temperatures $T_C$ of various samples were derived from ac and dc magnetic susceptibility measurements. $T_C$ values of both as-prepared $Ni_3Sn_2$ (LTP) and quenched $Ni_3Sn_2$ (HTP) are approximately 5 K. Hardly any influence of ball milling on the Curie temperature is found.

The thermal stability of $Ni_3Sn_2$ after various periods of milling was studied by DSC. Typical DSC scans after various periods of milling are given in Fig. 16, where the scan of the quenched material is also shown. The DSC scan of the starting compound (0 h) exhibits an endothermic peak at 786 K. This corresponds to the equilibrium phase transition to the HTP. The transition temperature of 786 K is lower than the 873 K expected from the phase diagram.[22] This endothermic peak also appears in all ball-milled samples. The heat consumed in the endothermic transition is plotted in Fig. 17 (open circles) as a function of milling time. The heat involved in this transition decreases with milling time in the early stage of milling. After milling for periods longer than 50 h it tends to become constant with a heat content of about 2 kJ/mol. The peak temperature of this transition decreases from 786 to 766 K after milling from 0 to 100 h (Fig. 18, open circles). Furthermore a broad exothermic peak in the temperature range 400–600 K is detectable after milling periods from 8 to 100 h. This peak becomes more pronounced with increasing milling time. The heat content increases to about 4 kJ/mol for milling periods longer than 40 h. Another exothermic peak at about 620 K is also detectable after milling for 8 h. This peak becomes much more pronounced after 40 h of milling. The heat evolved in this transition is also plotted in Fig. 17 (open squares). The heat increases with milling time. A drastic increase is found after 40 h of milling. The heat effect tends to saturate upon further milling and becomes 1.36 kJ/mol after 50 h, up to 100 h of milling. The peak temperature increases with milling time as can be seen in Fig. 18 (open squares). The shape of this peak is very similar to the exothermic peak appearing in the quenched

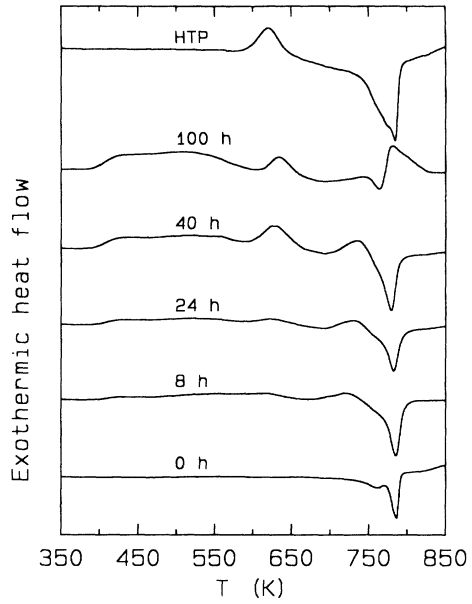


FIG. 16. Typical DSC scans of $Ni_3Sn_2$ after milling for various periods, as well as that of the high-temperature phase $Ni_3Sn_2$ quenched from 1073 K (top curve marked as HTP).

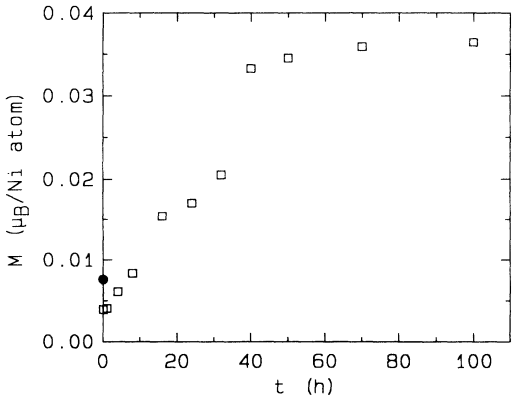


FIG. 15. Magnetization at 4.2 K of $Ni_3Sn_2$ at 21 T as a function of milling time. The filled circle at zero hour of milling denotes the magnetization of the high-temperature phase of $Ni_3Sn_2$ quenched from 1073 K.

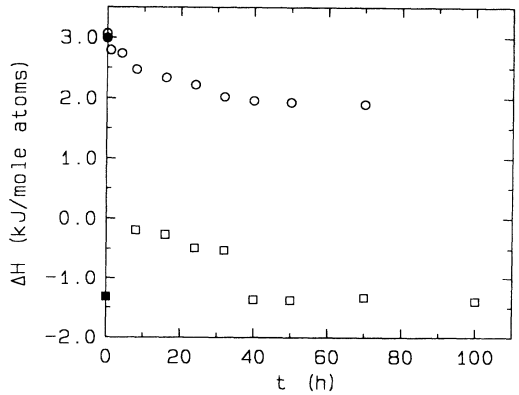


FIG. 17. Heat content in the endothermic transition (open circles) and in the exothermic transition of the phase restoration (open squares) in $Ni_3Sn_2$ as a function of milling time. The filled symbols at zero hour of milling denote the heat content in the respective transitions of the $Ni_3Sn_2$ quenched from 1073 K (HTP).

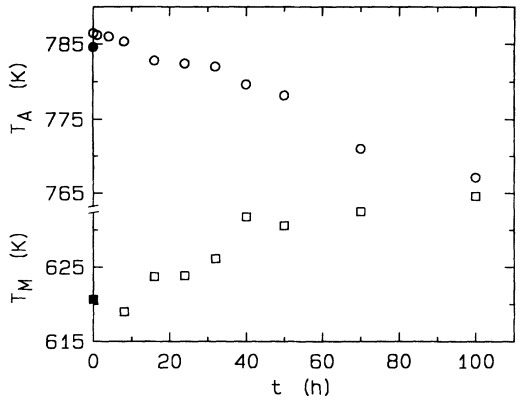


FIG. 18. Endothermic transition temperature ($T_A$) in various ball-milled $Ni_3Sn_2$ samples (open circles) and the transition temperature ($T_M$) of phase restoration (HTP to LTP) (open squares) as a function of milling time. The filled symbols at zero hour of milling denote the peak temperatures in the respective transitions of $Ni_3Sn_2$ quenched from 1073 K (HTP).

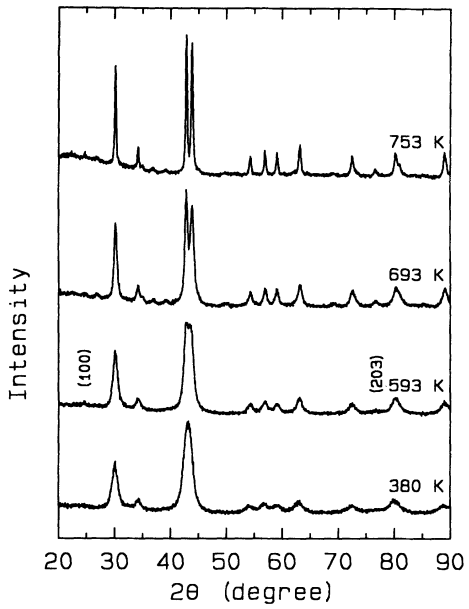


FIG. 19. X-ray-diffraction patterns of $Ni_3Sn_2$ milled for 100 h after heating in the DSC to various temperatures and subsequently cooling to room temperature at a cooling rate of 200 K/min.

HTP (top curve in Fig. 16). It should also be noted that starting from the sample milled for 8 h another exothermic peak is observed at 720 K. It becomes more pronounced upon further milling. The heat evolved in this transition is estimated as 1.1 kJ/mol for samples milled for 40 and 50 h. The DSC scan of the HTP quenched from 1073 K (top curve in Fig. 16) shows similar behavior as in the samples milled for a long time. Here, only one single exothermic peak at a temperature of 620 K and one endothermic peak at a temperature of about 784 K are observed. The exothermic peak corresponds to the transformation of the metastable HTP to the equilibrium LTP (phase restoration). The peak temperature of the exothermic transition is lower than that of the second exothermic transition in the samples after long periods of milling (see Fig. 18). The heat evolved in the exothermic transition is derived as 1.32 kJ/mol (filled square at zero hour of milling in Fig. 17), which is almost the same as that in the second exothermic transition of the materials milled longer than 32 h (open squares in Fig. 17). In contrast, the temperature of the endothermic transition (filled circle at zero hour of milling in Fig. 18) is higher than that for the samples milled for long periods and the transition heat (filled circle at zero hour of milling in Fig. 17) is larger. Moreover, for the quenched sample the transition temperature and transition heat are quite close to the original transition peak for the starting material.

Figure 19 shows the x-ray-diffraction patterns of $Ni_3Sn_2$ milled for 100 h after heating to different temperatures. The pattern indicated by 380 K, the starting temperature of the broad exothermic transition, does not show any change. The pattern marked 593 K, the end temperature of the broad exothermic peak, is still characteristic of the hexagonal HTP but has two extra reflections, i.e., (100) and (203), and sharper Bragg peaks. The pattern labeled 693 K, the end of the second exothermic peak, is characteristic of the orthorhombic LTP. After further heating to 753 K, the pattern is still characteristic of the LTP, but the peaks are much sharper than those of the sample heated to 693 K. The temperature of 753 K is below the equilibrium transition temperature and in the last exothermic peak. Kissinger[19] plots (5, 10, 20, and 40 K/min) are displayed in Fig. 20 for the first and second exothermic peaks after 100 h of milling. The activation energies are 112 kJ/mol for the first and 156 kJ/mol for the second peak.

## IV. GENERAL DISCUSSION

First, let us discuss the change in magnetization. As mentioned earlier, in the equilibrium hexagonal HTP of $Ni_3Sn_2$, $Fe_3Ge_2$, and $Mn_3Sn_2$ all of the I sites and only half of the II sites are occupied. The LTP of $Ni_3Sn_2$ is

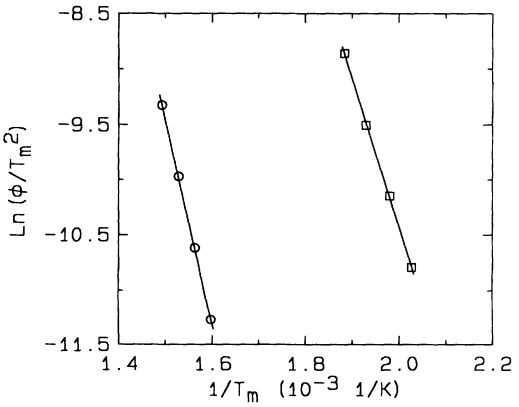


FIG. 20. Kissinger plots for the first (broad) exothermic transition (squares) and the second exothermic peak (circles) in $Ni_3Sn_2$ milled for 100 h in DSC. $\phi$ is the heating rate and $T_m$ the peak temperature.

very similar to the HTP, only the atoms are shifted somewhat from their positions to form an orthorhombic structure. In the equilibrium state, the total magnetization of these compounds is

$$M=\tfrac{1}{3}(2M_{T\mathrm{I}}\pm 1M_{T\mathrm{II}}) , \quad (1)$$

where $M_{T\mathrm{I}}$ is the spin moment per $T$ (transition-metal) atom on I sites and $M_{T\mathrm{II}}$ is the spin moment per $T$ atom on II sites. The factors 2 and 1 account for the occupancies of the respective sites. The plus sign on the right-hand side is for the *ferro*magnetic compounds, whereas the minus sign holds for *ferri*magnetic compounds. If during ball milling the transition-metal atoms jump from I sites to II sites, the magnetization changes as follows,

$$M=\tfrac{2}{3}[(1-C)M_{T\mathrm{I}}\pm(\tfrac{1}{2}+C)M_{T\mathrm{II}}] , \quad (2)$$

where $C$ is the fraction of $T$ atoms transferred. By neutron diffraction on $B8_2$-structure Fe-Ge and Mn-Ge[23] and in similar orthorhombic compounds[24] it was found that the magnetic moment of atoms on II sites is always larger than of atoms on I sites. The reason is a difference in interatomic distances and nearest-neighbor configuration. Moreover, the $Ni_3Sn_2$ and $Fe_3Ge_2$ are ferromagnetic[15,20] (parallel spin moments on I and II sites), whereas $Mn_3Sn_2$ is ferrimagnetic [25,26] (antiparallel spin moments). Thus, the plus sign in the right-hand side of Eqs. (1) and (2) holds for $Ni_3Sn_2$ and $Fe_3Ge_2$, whereas the minus sign holds for $Mn_3Sn_2$ If during ball milling an increasing fraction $C$ of atoms is transferred from I to II sites, the magnetization of $Ni_3Sn_2$ and $Fe_3Ge_2$ will increase, whereas it will decrease in $Mn_3Sn_2$. This is corroborated by the experiment. Milling $Ni_3Sn_2$ longer than 40 h, $Fe_3Ge_2$ longer than 140 h, and $Mn_3Sn_2$ longer than 60 h results in a constant magnetization as a function of milling time. Then apparently the net transfer of atoms stops and a stationary state is reached. However, the crystallite size of $Mn_3Sn_2$ is still being refined upon further milling. The drop of the magnetization of $Mn_3Sn_2$ after 120 h of milling may be due to this effect. The abrupt increase in magnetization in LTP $Ni_3Sn_2$ after 40 h of milling (Fig. 15) is due to a mechanically induced phase transformation from the orthorhombic LTP to the $B8_2$-type hexagonal HTP. (Evidence for such a phase transformation was obtained from the x-ray-diffraction patterns as shown in Fig. 14. Further evidence came from the analysis of the DSC scans of ball-milled $Ni_3Sn_2$ in comparison with the HTP obtained by rapid quenching.) The filled circle at zero hour of milling in Fig. 15 denotes the magnetization of the HTP quenched from 1073 K. The value is higher than that of the ordered LTP (open square at zero hour of milling). So an increase of the magnetization is expected during the LTP→HTP transformation. It is interesting that the magnetization of the HTP obtained by ball milling is much higher than that of the HTP obtained by quenching. This is explained as follows: the atoms transferred from I sites to II sites during ball milling of the LTP remain there after the phase transformation and these atoms have in both phases a higher magnetic moment. In order to check if disordering between I and II sites also occurs at higher temperatures, we quenched $Ni_3Sn_2$ from various high temperatures (973, 1073, and 1173 K). It turned out that in all the quenched samples the magnetization behavior did not change. Either our quenching rate is too low ($10^4$ K/s) or there is no such disorder at high temperature.

The increase of unit-cell volume of these compounds is compatible with the atomic transfer of the transition-metal atoms from I to II sites. The volume of octahedral interstices (I) is larger than that of tetrahedral interstices (II). If the atoms on I sites really jump to II sites during ball milling, a volume expansion is expected, for the following reason. When an atom jumps from a I site to a II site, a I site is emptied, whereas a II site is filled. Stress relaxation around the vacant I site will lead to a decrease of the unit-cell volume ($\Delta V_o$). However filling of a II site will probably lead to a stronger increase of the unit-cell volume ($\Delta V_i$). This means an increase in unit-cell volume since $\Delta V=\Delta V_i-\Delta V_o$ is then positive. This is what is experimentally observed. This is another indication that transition-metal atoms are really displaced. It was found by us[15] that the unit-cell volume of ball-milled HTP $Ni_3Sn_2$ is about 1% larger than that of quenched HTP $Ni_3Sn_2$. This supports the conclusion that the Ni atoms transferred during ball milling of the LTP remain on the II sites after the phase transformation, whereas in the quenched HTP such a redistribution does not exist.

The Curie temperature $T_C$ of $Mn_3Sn_2$ shown in Fig. 6 decreases continuously with milling time. After 60 h of milling, the $T_C$ value tends to become constant. The change of $T_C$ results mainly from atomic displacements. This can be explained as follows: For the transition-metal–tin intermetallics with $B8_2$-type structure it has been pointed out that, among the exchange interactions of two transition-metal atoms on I sites $J_{11}$, on a I site and a II site $J_{12}$, and on two II sites $J_{22}$, the exchange interaction $J_{12}$ is predominant, and that the Curie temperature is determined by this quantity.[25] Judged by the superlattice reflections, the $Mn_{\mathrm{II}}$ atoms and holes are distributed in a long-range-ordered (LRO) way over the II positions. The superexchange interaction between Mn atoms on I sites and on II sites may play an important role in determining the Curie temperature of $Mn_3Sn_2$. In the early state of milling the intensity of the superlattice reflections decreases sharply and they disappear after 30 h of milling. Apparently this LRO is lost. At the same time $T_C$ decreases sharply. This is naturally attributed to a decrease of $J_{12}$ by loss of LRO. On further milling $T_C$ is still decreasing. For the explanation let us express $T_C$ in the mean-field approximation as

$$3k_BT_C=a_{11}+a_{22}+[(a_{11}-a_{22})^2+4a_{12}a_{21}]^{1/2} . \quad (3)$$

$a_{xy}$ represents the magnetic energy between the $x$ and $y$ spins (1 stands for I and 2 stands for II) and $k_B$ is the Boltzmann constant. Neglecting here the relatively weak $T_{\mathrm{I}}$-$T_{\mathrm{I}}$, $T_{\mathrm{II}}$-$T_{\mathrm{II}}$ exchange energies,

$$3k_BT_C=(4a_{12}a_{21})^{1/2} , \quad (4)$$

where

$$a_{12}a_{21}=\frac{N_1}{N_t}\frac{N_2}{N_t}Z_{12}Z_{21}S_1(S_1+1)S_2(S_2+1)J_{12}^2 \ . \quad (5)$$

$N_t$ is the total number of atoms per formula unit $T_3X_2(N_t=5N)$, $N_i$ the number of transition metal atoms on $i$ sites, and $Z_{ij}$ the number of their nearest neighbors on $j$ sites. $S_i$ is the so-called pseudospin for the $3d$ electrons obtained via the observed atomic $3d$ magnetic moment $M_i=g_T\mu_B S_i$ ($g_T$ is the Landé factor, $\mu_B$ the Bohr magneton); and $J_{ij}$ the exchange interaction constant between $i$ and $j$ sublattices.

In $T_3X_2$, $N_1=2N$, $N_2=N$, $N_X=2N$, and $Z_{12}=3$, whereas $Z_{21}=6$. If during ball milling $n$ atoms are transferred from I sites to II sites then $N_1=2N-n$, $N_2=N+n$, $Z_{12}=6(\frac{1}{2}+n/2N)$, and $Z_{21}=6(1-n/2N)$. Let

$$S(S+1)=\sqrt{S_1(S_1+1)S_2(S_2+1)} \ . \quad (6)$$

Substituting $N_1$, $N_2$, $Z_{12}$, and $Z_{21}$, Eq. (5) becomes

$$a_{12}a_{21}=\frac{(2N-n)}{5N}\frac{(N+n)}{5N}6\left[\frac{1}{2}+\frac{n}{2N}\right]\times 6\left[1-\frac{n}{2N}\right][S(S+1)J_{12}]^2 \ . \quad (7)$$

Combining Eqs. (4) and (7), we obtain

$$3k_BT_C=\frac{12}{5}\left[1+\frac{n}{2N}-2\left[\frac{n}{2N}\right]^2\right][S(S+1)J_{12}] \ . \quad (8)$$

Let $C=n/2N$ be the fraction of I atoms transferred to II sites; then we obtain

$$T_C=\frac{4J_{12}(1+C-2C^2)S(S+1)}{5k_B} \ , \quad (9)$$

where $S$ is obtained from Eq. (6) as

$$S=[1+4\sqrt{S_1S_2(S_1+1)(S_2+1)}]^{1/2}-1 \ . \quad (10)$$

Thus, $T_C$ after ball milling is determined by Eq. (9). Due to the atomic displacements from I sites to II sites upon further milling, the fraction of Mn atoms going from I sites to II sites is increasing. This will lead to an increase of the term $(1+C-2C^2)$ in Eq. (9) because $0\le C\le 0.5$. If we assume that the value of $J_{\text{Mn-Mn}}$ does not change any more upon milling, there will be an increase in $T_C$ value. However, it was experimentally observed that the $T_C$ value of $Mn_3Sn_2$ still decreases gradually upon further milling, which means that, in fact, the exchange interaction constant $J_{\text{Mn-Mn}}$ is decreasing with increasing milling time in the later stage of milling. In $Ni_3Sn_2$ the Curie temperature is constant. This is also due to the decrease of the Ni-Ni exchange interaction constant $J_{12}$. The effect of increase of the $C$ value is apparently compensated by a decrease of $J_{12}$. The gradual decrease of the Curie temperature of $Mn_3Sn_2$ in the later stage of milling indicates that the decrease of the exchange interaction constant $J_{12}$ in $Mn_3Sn_2$ is stronger than in $Ni_3Sn_2$.

We proceed to the DSC results. From the x-ray-diffraction patterns shown in Fig. 9, it is clear that the first exothermic transition in the ball-milled $Mn_3Sn_2$ corresponds to the release of internal stresses and an increase of the short-range ordering (SRO). The second peak in the DSC scans corresponds to the development of atomic reordering from the short-range-ordered state to the originally long-range-ordered state. As already mentioned, in the perfect compound there is a long-range-ordered arrangement of the holes and Mn atoms on II sites. The third exothermic peak is due to the growth of nanocrystallites. The same conclusions apply to $Fe_3Ge_2$. The heat evolved in the atomic reordering process increases with milling time. The tendency is consistent with the variation of unit-cell volume and magnetization. The activation energies for the atomic reordering are 174 kJ/mol for the first peak and 102 kJ/mol for the second peak in ball-milled $Mn_3Sn_2$. The activation energy for ball-milled $Fe_3Ge_2$ is about 103 kJ/mol, which is quite close to that in $Mn_3Sn_2$ (second peak). The total heat evolved in the exothermic transitions in both $Mn_3Sn_2$ and $Fe_3Ge_2$ milled for a long time is approximately 4 kJ/mol. From the x-ray-diffraction patterns shown in Fig. 19, it is clear that the broad exothermic transition (first exothermic peak) in $Ni_3Sn_2$ milled for various periods corresponds to the increase of atomic ordering and the release of internal stresses. This provides further evidence that the ball-milled LTP as well as the ball-milled HTP is atomically disordered. The broad character of this transition reflects a similar process of atomic reordering in $Ni_3Sn_2$ to that in $Mn_3Sn_2$ and $Fe_3Ge_2$. In fact it includes two overlapping peaks as can be seen in Fig. 16, especially for the sample milled for 100 h. The total heat evolved in this peak is also about 4 kJ/mol after long periods of milling. The activation energy is calculated as 112 kJ/mol for the peak at about 500 K. The absence of such an exothermic transition in the quenched HTP again proves that the particular type of atomic disorder cannot be generated by quenching from high temperatures. The second exothermic transition in the DSC scans of $Ni_3Sn_2$ after milling longer than 8 h corresponds to the phase restoration of the metastable HTP to the original equilibrium LTP, the same type of exothermic transition as in the quenched HTP. The heat evolved in the transition is about 1.36 kJ/mol for $Ni_3Sn_2$ milled longer than 40 h, which is almost the same as in the quenched HTP for the same type of transition. The last exothermic peak is responsible for the growth of the crystallites. This gives evidence that the ball-milled HTP has nanometer-scale crystallites. The heat evolved in the transition is about 1.1 kJ/mol for the samples after long periods of milling.

Theoretically, when a fully disordered intermetallic compound is heated, three major exothermic heat effects are expected: the relaxation of lattice defect and stresses and development of short-range order; the increase of long-range order; and crystallite growth from the nanocrystalline state to a microcrystalline state. In view of the required diffusion distances, these processes are expected to occur in the following sequence: SRO, LRO, and crystallite growth. The observation of three exothermic peaks in the heating process of the ball-milled $Mn_3Sn_2$, and $Fe_3Ge_2$ nicely illustrates the three stages de-

scribed above. Baro *et al.*[27] and Yavari *et al.*[28] have also observed three separate peaks in the DSC scans of ball-milled $Ni_3Al$. Furthermore, the observation of the third exothermic heat effect in $Mn_3Sn_2$ and $Fe_3Ge_2$ is similar to that measured by Eckert *et al.*[29] during nanograin growth in ball-milled nickel. However the third stage is not always observable. Since the transition temperatures of these transitions are too close to be separated, we can only derive the total heat evolved in the exothermic transitions. As already mentioned, the broad character of the first exothermic transition in ball-milled $Ni_3Sn_2$ reflects a similar process of atomic reordering to that in $Mn_3Sn_2$ and $Fe_3Ge_2$. The method of atomic reordering in these ball-milled $T_3X_2$ compounds is as follows: during heating, $T$ atoms, which were transferred from I to II sites, will jump back to their original sublattice. The total heat released in the reordering process increases with milling time due to an increased transfer of atoms from I to II sites. The total energies stored in $Mn_3Sn_2$ and $Fe_3Ge_2$ are approximately 4 kJ/mol, whereas the total energy stored in $Ni_3Sn_2$ is about 6.5 kJ/mol (the sum of the heat released during atomic reordering, phase restoration, and nanocrystallite growth). Estimates of differences of formation enthalpies between amorphous and crystalline material for $Ni_3Sn_2$, $Mn_3Sn_2$, and $Fe_3Ge_2$ are 13, 13, and 2.6 kJ/mol, respectively.[30,31] Apparently, the total energy stored in $Ni_3Sn_2$ and $Mn_3Sn_2$ is too low to drive the respective compounds from the crystalline state to the amorphous state. On the other hand, we have argued in Ref. 32 that antisite disorder may be the precondition for the formation of a solid solution or an amorphous state during ball milling. In these $B8$-like compounds, during ball milling only the transition-metal atoms redistribute over their own sublattice sites and there is no position exchange between transition-metal atoms and nontransition-element atoms. Such a redistribution of the transition-metal atoms does not destroy the "frame" of the structure. So, although the energy stored in $Fe_3Ge_2$ (4 kJ/mol) is higher than that required for the transformation from the crystalline to the amorphous state, the material remains in the crystalline state with disordered structure. This argument is also valid for $Ni_3Sn_2$ and $Mn_3Sn_2$.

Further support for the possibility of jumping of transition-metal atoms between I and II sites is obtained from tracer-diffusion experiments in $B8$ compounds.[33,34] The main diffusion mechanism that is inferred from those measurements involves jumping between I and II sites. The activation energy for tracer diffusion in various compounds of this type amounts to about 200 kJ/mol. This is twice the energy (102 kJ/mol in $Mn_3Sn_2$, 103 kJ/mol in $Fe_3Ge_2$, and 112 kJ/mol in $Ni_3Sn_2$) we attribute to the reordering process. In tracer diffusion the most difficult jumps in a sequence of jumps, i.e., the jumps with the highest activation energy, determine the diffusion speed. These are no doubt the I-to-II jumps. In contrast, in a reordering process we deal with II-to-I jumps, leading to a higher degree of atomic order. Combining our results with those from Refs. 33 and 34, a tentative conclusion could be that I$\rightarrow$II jumps have an activation energy of about 200 kJ/mol and II$\rightarrow$I jumps have an activation energy of 100 kJ/mol.

Let us discuss the phase transformation in $Ni_3Sn_2$. Measurement of the exothermic heat effect evolved during phase restoration from the metastable HTP to the equilibrium LTP provides important information on the detailed process of phase transformation from the LTP to the HTP during ball milling. The appearance of this heat effect in the sample milled for 8 h indicates that the phase transformation starts at a milling time of 8 h. However, it develops very slowly during milling periods up to 32 h, as can be seen in Figs. 16 and 17. The transition heat increases slowly for milling periods up to 32 h and a drastic increase is observed after a milling time of 40 h. Then it tends to become constant upon further milling. This drastic increase at 40 h of milling is consistent with the abrupt increase of magnetization which also occurs at a milling time of 40 h. The fact that the heat effect in the sample after 32 h of milling is 37% of that in the sample milled for 40 h indicates that the phase transformation occurs mainly at a milling time of 40 h (the x-ray-diffraction pattern has the characteristics of the hexagonal-structure HTP at a milling time of 40 h). The material is a mixture of LTP and HTP in the milling periods from 8 to 32 h although the x-ray-diffraction pattern is still characteristic of the orthorhombic-structure LTP. The fact that the transition heat as well as the magnetization tends to become constant upon further milling indicates that the phase transformation is completed and the material is homogenized in the late stage of milling.

It is very interesting to note that the temperature of the endothermic transition from orthorhombic structure to hexagonal structure in the ball-milled LTP is lower than that in as-prepared $Ni_3Sn_2$ and the heat consumed in the transition in the ball-milled LTP is smaller than that in the original LTP (see Figs. 17 and 18). This reflects the fact that the disordered LTP is less stable than the order LTP. In contrast, the metastable disordered HTP obtained by ball milling is more stable than the metastable ordered HTP obtained by quenching. This is observed in Fig. 18, which shows that the temperature of the phase restoration from the metastable HTP to the equilibrium LTP in the ball-milled HTP is higher than that in the quenched HTP. So, we can conclude that atomic disorder induced by ball milling increases the stability of the hexagonal HTP and decreases the stability of the orthorhombic LTP. A peculiarity is that the special type of atomic disorder in the $B8_2$ structure cannot be generated by rapid quenching. Ball milling offers a unique technique to obtain the atomically disordered state.

Finally, it should be emphasized that the ball milling was carried out under continuous pumping in a vacuum of about $10^{-6}$ Torr. In this way reactions with nitrogen or oxygen were avoided. However, the milling was performed in a stainless-steel vial with a stainless-steel ball (but a tungsten carbide bottom). So iron impurities may be introduced. In order to check the quality of the samples, we annealed the long-time-milled samples and remeasured the physical properties, especially the magne-

tization. It turned out that the magnetization behavior and the value of the magnetization of the annealed samples are quite close to those of the initial compounds. The impurity iron content is less than 0.1 wt %.

Furthermore, it is noticed that the crystallite size of all the compounds studied decreases with increasing milling time and that nanocrystallites are formed in the late stage of milling. Crystallite size may influence the magnetization when the size is reduced to a few nanometers (5–6 nm). This is suggested as an explanation for the lower magnetization in $Mn_3Sn_2$ after 120 h of milling. However, the major changes in all physical parameters during milling occur in the early stage of milling, where the crystallite size is larger than 20–40 nm. These changes certainly result from the rearrangement of atoms in the crystalline structure induced by ball milling.

## V. CONCLUSIONS

Starting from ordered $Mn_3Sn_2$ and $Fe_3Ge_2$ compounds with $B8_2$-type hexagonal structure, mechanical milling generates well-defined atomic disorder of the type "redistribution of interstitials." This leads to an increase in magnetization in ferromagnetic $Fe_3Ge_2$, whereas it leads to a decrease in ferrimagnetic $Mn_3Sn_2$. These disordered materials remain in the $B8_2$ structure, but values of all physical parameters are far from those of the starting ordered compounds. The heat evolved in the atomic reordering process of both $Mn_3Sn_2$ and $Fe_3Ge_2$ after long-time milling is approximately 4 kJ/mol and the activation energy is about 100 kJ/mol. The volume expansion is 1.3% in $Mn_3Sn_2$ and 1.2% in $Fe_3Ge_2$ after long-time milling.

Starting from ordered $Ni_3Sn_2$ compounds with $Ni_3Sn_2$-type orthorhombic structure (LTP) mechanical milling also generates atomic disorder of the type "redistribution of interstitials" in the early stage of milling. The heat evolved in the atomic reordering process and activation energy is 4 and 112 kJ/mol, respectively. After long milling times the compound transforms to the $B8_2$-type hexagonal structure (HTP) as at higher temperature in the phase diagram. The magnetization of the HTP obtained by ball milling is much higher than that obtained by quenching. This is due to atomic disorder in the ball-milled HTP. The Ni atoms which were redistributed over the two different interstices during ball milling of the LTP remain there after the phase transformation. The heat evolved in the phase restoration of the metastable disordered HTP to the equilibrium ordered LTP and the activation energy are 1.36 and 156 kJ/mol, respectively.

The particular type of atomic disorder induced by ball milling cannot be generated by rapid quenching from high temperature. The disorder increases the stability of HTP $Ni_3Sn_2$ and decreases the stability of LTP $Ni_3Sn_2$. It is also clear that atomic disorder is the main source of energy storage during ball milling of intermetallic compounds. The energy stored in the grain boundaries is much lower than that stored in atomic disorder.

## ACKNOWLEDGMENTS

We gratefully acknowledge the Dutch Foundation for Fundamental Research on Matter (FOM) for financial support.

[1]A. Y. Yermakov, Y. Y. Yurchikov, and V. A. Barinov, Fiz. Met. Metalloved. **52**, 50 (1981); **54**, 90 (1982).
[2]R. B. Schwarz and C. C. Koch, Appl. Phys. Lett. **49**, 146 (1986).
[3]A. W. Weeber, H. Bakker, and F. R. de Boer, Europhys. Lett. **2**, 445 (1986).
[4]M. S. Kim and C. C. Koch, J. Appl. Phys. **62**, 3450 (1987).
[5]H. Bakker and L. M. Di, in *Mechanical Alloying*, Vols. 88-90 of Materials Science Forum, edited by P. H. Shingu (Trans Tech, Aedermannsdorf, Switzerland, 1992), p. 27.
[6]D. L. Beke, H. Bakker, and P. I. Loeff, Acta Metall. Mater. **39**, 1267 (1991); **39**, 1259 (1991).
[7]C. Massobrio, V. Pontikis, and G. Martin, Phys. Rev. Lett. **62**, 1142 (1989).
[8]W. L. Johnson, Prog. Mater. Sci. **30**, 81 (1986).
[9]R. B. Schwarz and R. R. Petrich, J. Less-Common Met. **140**, 171 (1988).
[10]C. C. Koch, J. S. C. Jang, and P. Y. Lee, in *New Materials by Mechanical Alloying Techniques*, edited by E. Arzt and L. Schultz (DGM Infromationsgesellschaft, Oberursel, 1989), p. 101.
[11]L. M. Di, P. I. Loeff, and H. Bakker, J. Less-Common Met. **168**, 183 (1991).
[12]L. M. Di and H. Bakker, J. Appl. Phys. **71**, 5650 (1992).
[13]L. M. Di, H. Bakker, Y. Tamminga, and F. R. de Boer, Phys. Rev. B **44**, 2444 (1991).
[14]L. M. Di, H. Bakker, and F. R. de Boer, Physica B **182**, 91 (1992).
[15]G. F. Zhou, L. M. Di, and H. Bakker, J. Appl. Phys. **73**, 1521 (1993).
[16]G. F. Zhou and H. Bakker, Phys. Rev. B **48**, 7672 (1993).
[17]A. J. Riemersma, R. J. D. Manuputy, H. Schlatter, W. F. Moolhuyzen, R. Rik, D. M. R. Lo Cascio, and P. I. Loeff, Rev. Sci. Instrum. **62**, 1084 (1991).
[18]R. Gersdorf, F. R. de Boer, J. C. Wolfrat, F. A. Muller, and L. W. Roeland, in *High-Field Magnetism*, edited by M. Date (North-Holland, Amsterdam, 1983), p. 277.
[19]H. E. Kissinger, Anal. Chem. **29**, 1702 (1957).
[20]K. Kanematsu, and T. Ohoyama, in *Proceedings of the International Conference on Magnetism*, Nottingham, 1964 (Institute of Physics and Physical Society, London, 1964), p. 512.
[21]P. Villars and L. D. Calvert, *Pearson's Handbook of Crystallographic Data for Intermetallic Phases* (American Society for Metals, Metals Park, OH, 1986), p. 2897.
[22]T. B. Massalski, *Binary Alloy Phase Diagrams* (American Society for Metals, Metals Park, OH, 1986), p. 1759.
[23]J. B. Forsyth and B. J. Brown, in *Proceedings of the International Conference on Magnetism* (Ref. 20), p. 524.

[24]O. Beckman and L. Lundgren, in *Handbook of Magnetic Materials,* edited by K. H. J. Buschow (North-Holland, Amsterdam, 1991), Vol. 6, p. 224.
[25]M. Asanuma, J. Phys. Soc. Jpn. **17**, 300 (1962).
[26]H. Potter, Philos. Mag. **12**, 255 (1931).
[27]M. D. Baro, J. Malagelada, S. Surinach, N. Clavaguera, and M. T. Clavaguera-mora, in *Ordering and Disordering in Alloys,* edited by A. R. Yavari (Elsevier, Applied Science, London, 1992), p. 65.
[28]A. R. Yavari, P. Crespo, E. Pulido, A. Hernando, G. Fillion, P. Lethuillier, M. D. Baro, and S. Surinach, in *Ordering and Disordering in Alloys* (Ref. 27), p. 12.
[29]J. Eckert, J. C. Holzer, C. E. Krill, and W. L. Johnson, in *Mechanical Alloying* (Ref. 5), p. 505.
[30]F. R. de Boer, R. Boom, W. C. M. Mattens, A. R. Miedema, and A. K. Niessen, *Cohesion in Metals, Transition Metal Alloys,* edited by F. R. de Boer and D. G. Pettifor (North-Holland, Amsterdam, 1988).
[31]H. Yang and H. Bakker, J. Alloys Compounds **189**, 113 (1992); (unpublished).
[32]H. Bakker, L. M. Di, H. Yang, and G. F. Zhou, in *Mechanical Alloying for Structural Applications,* edited by J. J. de Barbadillo, F. H. Froes, and R. Schwarz (American Society for Materials, Metal Park, OH, 1993), p. 213.
[33]H. Schmidt, G. Frohberg, and H. Wever, Acta Metall. Mater. **40**, 3105 (1992).
[34]H. Frohberg and H. Wever, in *Ordered Intermetallic,* edited by C. T. Liu, R. W. Cahn, and G. Sauthoff (Kluwer, Dordrecht, 1992), p. 496.